Terahertz generation by means of ZnGeP$_2$ large aperture photoconductive antenna

Vladislava Bulgakova ,[a,*] **Aleksandr Ushakov** ,[a] **Pavel Chizhov** ,[a]
Nikolay Yudin,[b,c,d] **Mikhail Zinovev,**[b,c,d] **Sergey Podzyvalov,**[b,c,d]
Timophey Dolmatov,[a] **Vladimir Bukin** ,[a] **and Sergey Garnov**[a]

[a]Prokhorov General Physics Institute of the Russian Academy of Sciences, Moscow, Russia
[b]National Research Tomsk State University, Tomsk, Russia
[c]V. E. Zuev Institute of Atmospheric Optics SB RAS, Tomsk, Russia
[d]LLC "Laboratory of Optical Crystals," Tomsk, Russia

Abstract. The generation of terahertz (THz) radiation using a ZnGeP$_2$ (ZGP) large-aperture photoconductive antenna (PCA) was demonstrated. The semiconductors were excited above and below the bandgap (400 and 800 nm) by a femtosecond Ti:sapphire laser. The THz pulse waveform generated by the ZGP antenna was measured using a time-domain spectroscopy technique. The antenna's THz pulse energy dependence on the optical pump energy was measured, and saturation fluence and carrier mobility were estimated. The ZGP and a chemical vapor deposited ZnSe-based PCA were compared. © *2021 Society of Photo-Optical Instrumentation Engineers (SPIE)* [DOI: 10.1117/1.OE.60.8.082015]

Keywords: ZnGeP$_2$; photoconductive antenna; large-aperture photoconductive antennas; terahertz radiation; time-domain measurements; two-photon absorption.

1 Introduction

Photoconductive antennas (PCAs) are promising sources of relatively high energy terahertz (THz) pulses. Another advantage of such sources is their potential to generate asymmetric THz pulses with a low-frequency part and high ponderomotive potentials.[1] There are different types of PCA substrate materials; the most common are GaAs,[2] ZnSe,[3] and 6H-SiC.[4] With a 1.44-eV bandgap, GaAs can be excited by a Ti:sapphire (Ti:Sa) laser fundamental harmonic and is widely used as a PCA substrate due to its high carrier mobility ($\mu_n \approx 3000 \; \text{cm}^2/\text{V} \cdot \text{s}$ at 300 K).[5] The use of ZnSe ($\mu_n \approx 400 \; \text{cm}^2/\text{V} \cdot \text{s}$ at 300 K)[5] with a bandgap of 2.7 eV allows for the application of higher bias fields due to a higher dielectric discharge threshold. Furthermore, ZnSe can be excited by a Ti:Sa laser at the fundamental and second harmonics above (400 nm) and below (800 nm) the bandgap.[3] Recently, 6H-SiC ($\mu_n \approx 480 \; \text{cm}^2/\text{V} \cdot \text{s}$ at 300 K)[5] 3.03-eV bandgap crystal was investigated as a PCA substrate.[4] It can be excited by the second harmonic of a Ti:Sa laser and has superior thermal properties compared to ZnSe.[4,6]

Chalcopyrite ZnGeP$_2$ (ZGP) is widely used as nonlinear optical media in the mid-IR and THz range.[7–10] However, this material has not been previously used as a PCA substrate. The bandgap energy of ZGP is 2.2 eV, which makes it possible to excite this media above the bandgap not only by the second harmonic of Ti: Sa systems but also by the second harmonic of Yb-based femtosecond lasers (Yb:KGW and Yb-fiber lasers). Therefore, Yb-based femtosecond lasers with the ZGP antenna could provide more compact devices for THz applications. The ZGP[11] has a higher THz transparency than chemical vapor deposited-ZnSe[12] (CVD-ZnSe), which is an advantage of using this material as a PCA substrate. In addition, the dielectric breakdown threshold of ZGP is higher or comparable to that of ZnSe. This property allows for high bias voltages to be applied. In this study, we use ZGP as a semiconductor substrate for large-aperture photoconductive

*Address all correspondence to Vladislava Bulgakova, vbulgakova573@gmail.com

antennas (LAPCAs) and measure the parameters of such THz sources. We compare ZGP- and CVD-ZnSe-based LAPCAs.

2 Experimental Setup

The PCA is based on the ZGP single crystal with a diameter of 30 mm and a thickness of 5 mm. This crystal is grown vertically by the Bridgman method from a compound previously synthesized by the two-temperature method on a seed crystal with a (100) orientation.[13] The sample for experimental measurements is cut along the ingot in the form of a plane-parallel plate oriented parallel to the (001) plane. Both surfaces of the test piece are optically polished. The free hole concentration is $\sim 2.5 \times \cdot 10^{19}$ cm^{-3}.[14] Such crystals have a relatively high value of nonlinear susceptibility $d = 70 \cdot 10^{-12} - 85.4 \cdot 10^{-12}$ m/V and thermal conductivity (coefficient of 36 W/m · K).[15] The Maxwellian relaxation time of charge carriers ($\tau_m = 230$ ms) and the diffusion length of the photocarriers ($L_D = 1$ μm) for ZGP are measured in the article ($\mu\tau = 3.9 \times 10^{-8}$ cm^2/V).[16] The measured value of the ZGP surface breakdown field is 70 kV/cm, and the volume resistivity is $470 \cdot 10^6$ Ω · cm. The volume resistivity value is highly dependent on special preparation conditions. For comparison, the volume resistivity of ZnSe MOVPE film grown by the van-dar-Pauw technique at room temperature is 10^5 Ω · cm.[5]

Figure 1 shows the experimental setup used for the generation and detection of THz pulses. The Ti:Sa laser beam (Coherent Legend Elite, 3.2-mJ pulse energy, 1-kHz repetition rate, 130 fs duration, 800-nm center wavelength, and 10 mm beam diameter at a $1/e^2$) was split into two parts by a beamsplitter (BS). The first part passed through the BS and generated THz radiation in the LAPCA under investigation. In all of the experiments, the antennas consisted of a semiconductor substrate with aluminum tape electrical contacts. The electrodes, which had a longitudinal size of 12 mm, were deposited on the substrate sample surface 4 mm apart. The bias voltage pulse with an amplitude $Ub = 2$ kV (which corresponds to a bias field of $Eb = 5$ kV/cm) and duration of ~ 10 ns was applied by a high voltage (HV) pulse generator. The repetition rate of HV pulses was set to 500 Hz for lock-in detection to reduce laser-induced noise at 1 kHz.[17] The antenna was irradiated with the second harmonic radiation. A beta barium borate (BBO) crystal (I-type, 200 μm thickness) is used to provide second harmonic generation. The energy of the second harmonic pulses was 0.3 mJ. A Glan–Taylor polarizer was used to vary the energy of the optical pump pulse. An optical filter was used to absorb fundamental harmonic radiation.

In time-domain spectroscopy (TDS) experiments, the THz beam generated by the LAPCA was focused by a PTFE lens (f = 100 mm) to a ZnTe crystal (0.5-mm thickness, ⟨110⟩-cut). The reflected beam from the BS probe laser beam passed through a motorized delay line. It was used to measure the temporal dependence of the electric field strength of the THz pulse using electro-optical sampling. The THz waveform was recorded using a balanced detector connected to the lock-in amplifier.
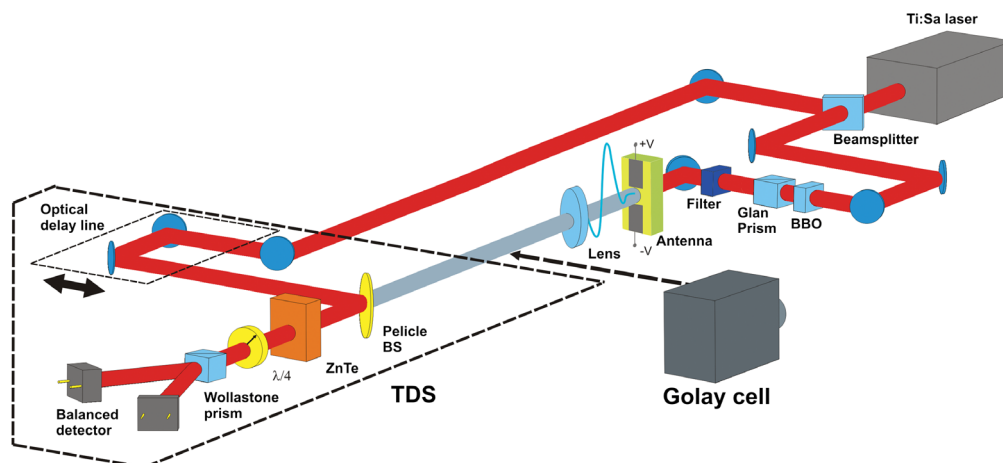

Fig. 1 Experimental setup for the generation and detection of THz pulses from a large-aperture PCA.

For the THz pulse energy measurements, a Golay cell (Tydex GC-1P) was used instead of the TDS system. In these experiments, laser radiation was gated with a 10-Hz frequency.

3 Results and Discussion

3.1 *Waveform and Energy Measurements of THz Emission*

The measured waveform of the electric field of the THz pulse generated in the ZGP LAPCA is shown in Fig. 2(a). A high-amplitude positive peak is observable in the THz pulse and a negative tail, the peak amplitude of which is smaller. Similar waveforms (with negative tails) have been previously observed for a ZnSe single-crystal LAPCA.[5] Using the Fourier transform, we obtained the spectrum of the THz pulse [Fig. 2(b)]. Spectral analysis revealed a peak at 0.5 THz, with no essential frequency components beyond 3 THz.

The THz pulse energy as a function of the optical excitation energy in ZGP LAPCA is shown in Fig. 3. The radiated THz pulse energy increased in a saturated manner with the rise of the optical pump energy. To estimate the saturation fluence of the ZGP substrate, taking into account the non-uniformity of the optical irradiation, we modeled the THz pulse energy dependence on the energy of optical excitation. Assuming that the optical beam intensity has a Gaussian distribution, the optical fluence is expressed by the following formula: $F(r) = (2W_{\mathrm{opt}}/\pi r_0^2) \cdot \exp(-2r^2/r_0^2)$, in which W_{opt} is optical energy and r_0 is the Gaussian beam radius at the $1/e^2$ level. The distribution of THz fluence is $F_{\mathrm{THz}}(r) = F(r) \cdot \eta(r)$. The proportionality factor between the optical and THz fluence is the conversion efficiency of the optical signal to THz (η):[18]
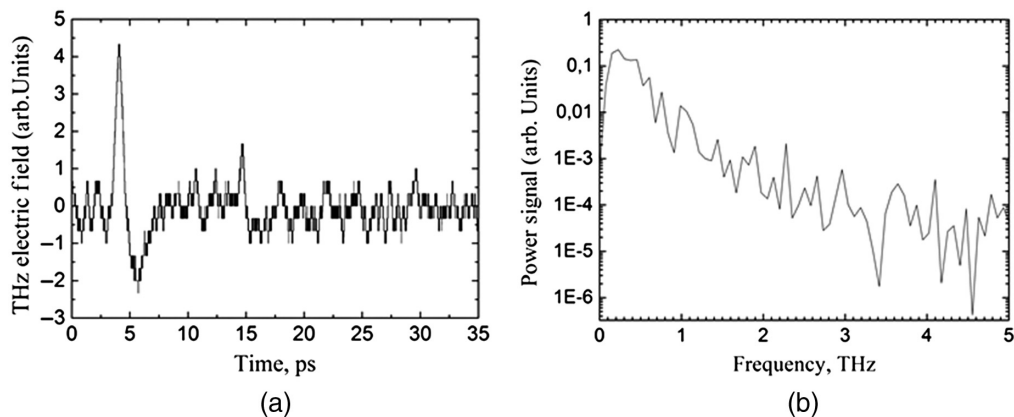

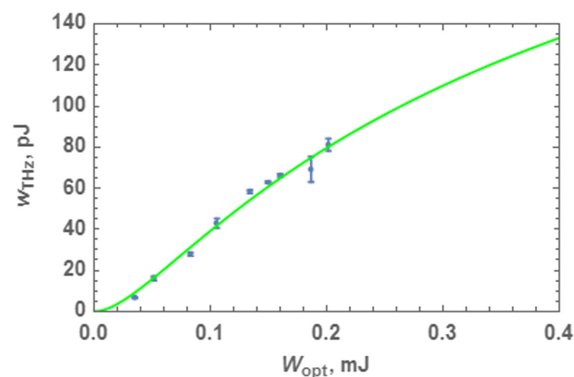**Fig. 2** The waveform of the THz pulse from the ZGP LAPCA.

Fig. 3 The ZGP LAPCA terahertz pulse energy as a function of optical excitation energy [experimental data (dots) and fitting (solid line)].

$$\eta = (\tau E_b^2 / 2FZ_0) \cdot \left(\frac{F}{F + F_{\text{sat}}} \right)^2,$$
(1)

in which τ is the THz pulse duration, E_b is the electric bias field, F is the optical fluence, and Z_0 is the free space impedance. $F_{\text{sat}} = h\upsilon(1 + n)/e\mu Z_0(1 - R)$[19] is the saturation fluence, corresponding to the fluence necessary to extract half of the maximum radiated field, in which $h\upsilon$ is the photon energy at the excitation wavelength; e is the electron charge; and n, μ, and R are the THz refractive index, the carrier mobility, and the optical reflection of the semiconductor substrate, respectively.

The total THz energy is

$$W_{\text{THz}} = \beta \int_S F_{\text{THz}}(r)\mathrm{d}S,$$
(2)

in which the integration region is the area between the electrodes (4×12 mm). The dimensionless factor β is included in Eq. (2) to account for the attenuation of THz pulse energy due to absorption in the antenna substrate, reflections, and other factors. In the calculations, we used the duration of a THz pulse $\tau = 1$ ps and the size of the 10-mm optical beam diameter at the $1/e^2$ level.

Figure 3 shows the experimental data and its best-fit line using Eq. (2) with variable F_{sat} and β parameters. The saturation fluence values ($F_{\text{sat}} = 0.27$ mJ/cm²) and $\beta = 0.022$ were obtained. To provide a comparison, we present the saturation fluence data for PCAs based on other substrates: $F_{\text{sat}} = 0.0105$ mJ/cm² for GaAs[5], $F_{\text{sat}} = 0.150$ mJ/cm² for ZnSe, and $F_{\text{sat}} = 0.24$ mJ/cm² for 6H-SiC. Taking into account the thickness of the ZGP antenna ($L = 0.5$ cm), the THz absorption coefficient $\alpha = 7.6$ cm⁻¹ could be estimated to correspond to the fitting attenuation factor of $\beta = 0.022$ [$\alpha = -\ln(\beta)/L$]. However, the calculated absorption coefficient differs from the known data:[11] $\alpha = 1$ cm⁻¹ at 1 THz. It can be assumed that other factors influence the difference between experimental and calculated values (which are related to an adjustment of the setup, among others). The optical refractive index of ZGP was $n \sim 3.5$,[20] and the reflection coefficient was $R \sim 0.3$. The refractive index of ZGP was $n = 3.4$ at 1 THz.[11] Using the value of the saturation fluence $F_{\text{sat}} = 0.27 \pm 0.13$ mJ/cm², we found the carrier mobility to be $\mu \approx 230 \pm 100$ cm²/V · s. The obtained mobility value differed from that reported by Sooriyagoda et al.[21] ($\mu \approx 150$ cm²/V · s), which could be attributed to different crystal growth techniques.

3.2 Pumping of the ZGP Antenna Above and Below the Bandgap

We conducted experiments to excite the ZGP antenna below (800 nm) the bandgap. Figure 4 shows the dependencies of the THz pulse energy versus the optical pump energy for the two excitation wavelengths [400 (see Sec. 3.1) and 800 nm]. The measured part of the optical energy
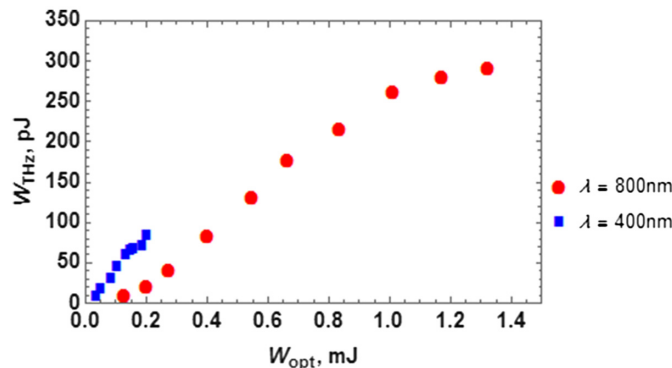

Fig. 4 The ZGP LAPCA THz pulse energy as a function of optical excitation energy for pumping above (400 nm) and below (800 nm) the bandgap.
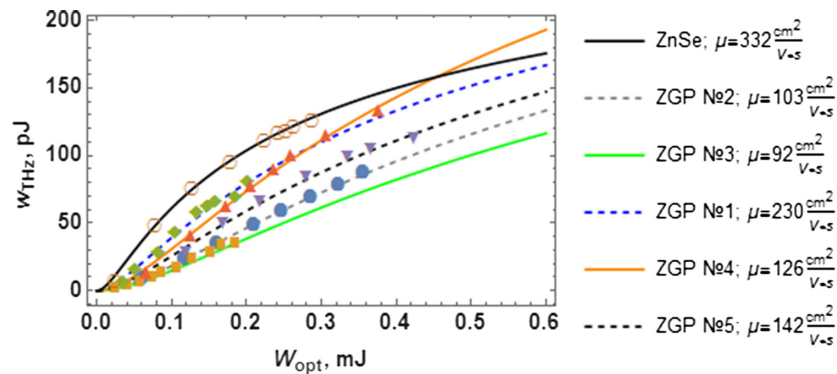
Fig. 5 The THz pulse energy as a function of optical excitation energy from LAPCA based on ZnSe and different ZGP materials.

transmitted through the antenna material at the wavelength of 800 nm was ∼1%. The bulk absorption of the laser radiation by the antenna material occurred on a scale comparable to or greater than the λ_{THz} in the medium. Figure 4 shows that, for the same optical energy values, a higher value of the THz pulse energy can be obtained when pumped at 400 nm.

3.3 ZGP Antennas with Different Impurities

We performed experiments to measure the dependencies of THz pulse energy versus optical pump energy for the antennas based on several ZGP substrate samples. All of these substrates were grown using the same method but with different amounts of residual synthesis components. In these experiments, the LAPCAs were excited at a 400-nm wavelength. Figure 5 shows the obtained experimental data and the approximation curves [constructed using Eq. (2)].

We compared the LAPCAs based on ZGP and the well-known ZnSe (with a thickness of $L = 0.5$ cm). The ZnSe antenna radiates THz pulses with more energy than the ZGP antenna with the same optical pump energy (Fig. 5). We found that the energy of the THz pulse of the ZnSe and ZGP antennas is comparable. Therefore, the carrier mobility in the material can vary between samples. The value of carrier mobility in these antennas varied in the range of $\mu \sim 92$ cm^2/V · s to $\mu \sim 230$ cm^2/V · s for ZGP.

4 Conclusions

We have demonstrated THz pulse generation with ZGP large-aperture PCAs excited above and below the bandgap. We obtained the THz pulse waveform, determined the dependence of THz pulse energy versus optical energy, and acknowledged the antenna materials' mobility. Optical pumping at 400 nm was more efficient. We found that the saturation fluence of the THz pulse of the ZGP antennas ($F_{sat} = 0.27$ mJ/cm^2) was comparable to that of the well-known ZnSe antenna ($F_{sat} = 0.13$ mJ/cm^2). However, a volume resistivity value higher than that for ZnSe allowed a larger bias field to be applied to the ZGP LAPCA. Therefore, the advantage of using the ZGP LAPCA is that the ZGP antenna can be pumped with a Yb-based femtosecond laser, and a high bias field can be applied.

Acknowledgments

References

1. X. Ropagnol et al., "Intense THz pulses with large ponderomotive potential generated from large aperture photoconductive antennas," *Opt. Express* **24**(11), 11299–11311 (2016).

2. M. Tani et al., "Emission characteristics of photoconductive antennas based on low-temperature-grown GaAs and semi-insulating GaAs," *Appl. Opt.* **36**(30), 7853–7859 (1997).

3. X. Ropagnol et al., "Toward high-power terahertz emitters using large aperture ZnSe photoconductive antennas," *IEEE Photonics J.* **3**(2), 174–186 (2011).

4. X. Ropagnol et al., "Improvement in thermal barriers to intense terahertz generation from photoconductive antennas," *J. Appl. Phys.* **116**, 043107 (2014).

5. O. Madelung, *Semiconductors: Data Handbook*, 3rd ed., Springer, New York (2003).

6. H. A. Hafez et al., "Intense terahertz radiation and their applications," *J. Opt.* **18**, 093004 (2016).

7. J. Cheng et al., "Synthesis and growth of $ZnGeP_2$ crystals: Prevention of non-stoichiometry," *J. Cryst. Growth* **362**, 125–129 (2013).

8. B. N. Carnio et al., "Terahertz electro-optic detection using a $\langle 012 \rangle$-cut chalcopyrite $ZnGeP_2$ crystal," *Appl. Phys. Lett.* **108**, 261109 (2016).

9. J. D. Rowley et al., "Terahertz emission from $ZnGeP_2$: phase-matching, intensity, and length scalability," *J. Opt. Soc. Am. B* **30**(11), 2882–2888 (2013).

10. Y. J. Ding and W. Shi, "Widely tunable monochromatic THz sources based on phase-matched difference-frequency generation in nonlinear-optical crystals: a novel approach," *Laser Phys.* **16**, 562–570 (2006).

11. K. Zhong et al., "Linear optical properties of $ZnGeP_2$ in the terahertz range," *Opt. Mater. Express* **7**(10), 3571–3579 (2017).

12. A. K. G. Tapia et al., "Charge carrier dynamics of ZnSe by optical-pump terahertz-probe spectroscopy," in *Int. Conf. Infrared, Millimeter, and Terahertz Waves*, IEEE (2011).

13. G. A. Verozubova, A. I. Gribenyukov, and Y. P. Mironov, "Two-temperature synthesis of $ZnGeP_2$," *Inorg. Mater.* **43**, 1040–1045 (2007).

14. S. D. Setzler, "Electron paramagnetic resonance and photoluminescence studies of point defects in zinc germanium phosphide ($ZnGeP_2$)," *Mater. Res. Soc. OPL* **450**, 327–332 (1996).

15. D. Nikogosyan, *Nonlinear Optical Crystals: A Complete Survey*, Springer, New York (2005).

16. P. Karavaev, V. M. Abusev, and G. A. Medvedkin, "Photorefractive effect in $ZnGeP_2$ single crystal," *Tech. Phys. Lett.* **32**(6), 498–500 (2006).

17. R. Yano, T. Hattori, and H. Shinojima, "Improvement of signal-to-noise ratio of terahertz electromagnetic waves by bias field modulation of photoconductive antenna," *Jpn. J. Appl. Phys.* **45**, 8714 (2006).

18. M. Reid and R. Fedosejevs, "Quantitative comparison of terahertz emission from (100) InAs surfaces and a GaAs large-aperture photoconductive switch at high fluences," *Appl. Opt.* **44**(1), 149–153 (2005).

19. P. K. Benicewicz and A. J. Taylor, "Scaling of terahertz radiation from large-aperture biased InP photoconductors," *Opt. Lett.* **18**(16), 1332–1334 (1993).

20. G. D. Boyd, E. Buehler, and F. G. Storz, "Linear and nonlinear optical properties of $ZnGeP_2$ and CdSe," *Appl. Phys. Lett.* **18**, 301 (1971).

21. R. Sooriyagoda et al., "Carrier transport and electron-lattice interactions of nonlinear optical crystals $CdGeP_2$, $ZnGeP_2$ and $CdSiP_2$," arXiv:2009.04605 (2020).

Vladislava Bulgakova is a PhD student at the Prokhorov General Physics Institute of the Russian Academy of Sciences. She received her BS and MS degrees in physics from Novosibirsk State Technical University in 2016 and 2018, respectively. The author of three papers and 12 conference presentations, she has experience in the field of THz plasmonics at the Novosibirsk Free Electron Laser.

Biographies of the other authors are not available.